















166 The tendency is clearer from 2008 to 2015, where all elevations saw a decrease in precipitation (-  
167 70, -120, -90, -168, -225 mm yr<sup>-1</sup> from LC to UCFL;  $r^2 = 0.51 - 0.70$ ), accentuated by a severe  
168 drought that took place in summer of 2015. The decreasing trend is then interrupted in 2017  
169 because of the high amount of precipitation caused by hurricane María. While our dataset is limited  
170 for analyzing climate trends, we can combine these observations to gauge how this variable is  
171 behaving as a function of time, as well as analyze short-term trends. The short-term trend seen in  
172 this study adjust to predictions of decreased precipitation in tropical forests as a consequence of  
173 climate change that have not been seen in previous studies for the Luquillo Mountains. While a  
174 richer dataset is required to assess changes in climatic patterns, short-term trends can highlight  
175 important features that deserves further observation.

176

#### 177 pH of Rainfall Samples

178 The pH had no relationship with elevation or rainfall volume, and in most instances, it remained  
179 within 5-6 for all elevation groups. The accepted value of unpolluted rainwater is 5.6 (Manahan,  
180 2000), slightly acidic because of the carbon dioxide to carbonic acid equilibrium reaction that takes  
181 place in the atmosphere/water interface. A pH lower or higher than this value could be influenced  
182 by acidic species from anthropogenic pollution, or by neutralizing species, like those found in  
183 mineral dust, respectively.

184

#### 185 Ionic Composition of Rainfall Samples

186 The mean annual weighted total ion concentration was studied as a function of time and grouped  
187 by elevation group. It showed that there was a tendency for higher ion concentrations in the



188 lowland stations, but it was not consistent through time. This relationship is tied up with increasing  
189 rainfall with elevation, which promotes a higher washout rate and a lower concentration of ions in  
190 the atmosphere and a more significant dilution caused by a higher volume of rainwater. Charge  
191 balance was examined as the slope of anions as a function of cations for all stations. Most stations  
192 had a slope higher than 1, which means there was a higher anion concentration than cations. A  
193 deviation from one suggests the presence of ions in the samples that the analytical procedure is  
194 unable to detect, which could be organic ions. The concentration of hydronium was calculated  
195 from pH measurements to identify if this was one of the missing cations. Still, it did not account  
196 for the lower concentration of cations relative to anions. The p-value for these regressions with a  
197 confidence interval of 95% was smaller than 0.0001 for all stations.

198 Ion concentration had a negative exponential relationship to rainfall, shown in Fig. 3. Pearson  
199 regression coefficient for the yearly values suggests that there is an inverse relationship between  
200 these variables for all years ( $r^2 = -0.66$  to  $-0.86$ ;  $n=159$ ) except for year 2013 ( $r^2 = -0.29$ ;  $n=20$ ).  
201 The poor relationship in 2013 is due to a value with low ion concentrations, that if omitted,  
202 improves the linear regression to an  $r^2 = -0.90$ . The concentration of ions is expected to decrease  
203 with an increasing volume of rain due to dilution and increased atmospheric particle washout,  
204 which validates the inverse relationship. The dilution effect followed a log-log linear relationship,  
205 and the p-values for all the regression coefficients were below 0.005 except for 2013, where it was  
206 0.211. Regression coefficients reveal that the tightness of this relationship is not constant and that  
207 large differences can occur. Most of these regression lines fall above the pure dilution line,  
208 suggesting that ion concentration is the dominant feature in the dilution process.

209

210 Seasonal Variation of Rainfall and Ionic Composition

211 The island of Puerto Rico is mainly affected by three aerosol types: marine, crustal, and  
212 anthropogenic, being  $\text{Na}^+$ ,  $\text{Ca}^{2+}$ , and  $\text{SO}_4^{2-}$  the proxy ions used for identifying the influence of  
213 these aerosols (McClintock et al., 2019; Stallard and Murphy, 2012). However, the presence of  
214  $\text{Ca}^{2+}$ , and  $\text{SO}_4^{2-}$  is not constant throughout the year and depends on seasonal patterns that transport  
215 aerosols from different sources. Sodium and sulfate ion concentrations were high during the first  
216 months of the year (Jan-Apr), which corresponds to the months with generally less rainfall (Fig.  
217 4). The increase in sulfate concentration is considerable during these months, particularly in  
218 lowland coastal, lowland interior, and lower montane stations, which could be caused by an  
219 enrichment of non-sea salt sulfate transported in anthropogenic aerosols from eastern United  
220 States by cold fronts. A bump in concentrations of the three ions is seen during the summer months  
221 of Jun-Aug, more drastically seen in the  $\text{Ca}^{2+}$  concentration. The cause of this could be an  
222 enrichment of non-sea salt calcium transported from the African continent by the trade winds and  
223 the position of the Intertropical Convergence Zone (ITCZ).

224 Since, in addition to the predominant  $\text{Na}^+$  and  $\text{Cl}^-$  both  $\text{Ca}^{2+}$  and  $\text{SO}_4^{2-}$  are found in sea salt particles,  
225 we assessed the marine influence of these ions per station calculating their Pearson correlation  
226 with  $\text{Na}^+$  (Table 2). A high correlation coefficient ( $>0.7$ ) was found between  $\text{Na}^+$  and  $\text{Cl}^-$  in 17 of  
227 the 21 stations, suggesting both these ions come from the same source for all stations, which is  
228 marine sea-salt particles. On the other hand,  $\text{Na}^+$  and  $\text{Ca}^{2+}$  were highly correlated in only one  
229 station (CDI), suggesting there is an important contribution of calcium from non-marine sources,  
230 the most important one being mineral dust from Africa.  $\text{Na}^+$  and  $\text{SO}_4^{2-}$  were highly correlated in  
231 13 out of 21 stations, suggesting that there is a substantial contribution of sulfate ions from marine  
232 sources. There is also a small but non-negligible contribution from non-marine sources, which

233 could be the contribution of anthropogenic pollution transported with cold fronts in the winter  
234 months.

235 Pearson correlation factor was analyzed for  $\text{Na}^{2+}$  and the non-sea salt fraction of  $\text{Ca}^{2+}$  and  $\text{SO}_4^{2-}$   
236 (Table 2). In some cases, especially in the lower stations, the correlation of  $\text{Na}^{2+}$  with  $\text{nss-Ca}^{2+}$   
237 was stronger than that of  $\text{Na}^{2+}$  with total  $\text{Ca}^{2+}$ . While  $\text{Na}^{2+}$  is mainly a marine aerosol, it is important  
238 to consider that it is also present in crustal sources, and this can be a possible explanation for this  
239 result. For higher elevation stations (LM, CFL, UCFL), the relationship of  $\text{Na}^{2+}$  with  $\text{nss-Ca}^{2+}$  was  
240 weaker than that of  $\text{Na}^{2+}$  with total  $\text{Ca}^{2+}$ . The weaker relationship could indicate that air masses  
241 containing crustal aerosols are less likely to reach higher elevation stations. The relationship of  
242  $\text{Na}^{2+}$  with  $\text{nss-SO}_4^{2-}$  was almost always weaker (19 out of 21 stations) than that of  $\text{Na}^{2+}$  with total  
243  $\text{nss-SO}_4^{2-}$  and in cases where it was higher, it was only slightly (less than 3% difference). This  
244 shows that  $\text{Na}^{2+}$  and  $\text{nss-SO}_4^{2-}$  have very distinct sources and that sources of  $\text{ss-SO}_4^{2-}$  and  $\text{nss-}$   
245  $\text{SO}_4^{2-}$  can be easily distinguished.

246

#### 247 Variations of Rainfall and Ionic Composition with Elevation

248 The ion mass deposition per unit area for all measured ion was determined for each elevation group,  
249 and the yearly average (Table 3). As expected,  $\text{Cl}^-$  and  $\text{Na}^+$  had the highest mass deposition for all  
250 stations, followed by  $\text{K}^+$ ,  $\text{SO}_4^{2-}$ ,  $\text{Ca}^{2+}$ ,  $\text{PO}_4^{3-}$ ,  $\text{Mg}^{2+}$ , and  $\text{NH}_4^+$ . Mass deposition of  $\text{NO}_3^-$ ,  $\text{F}^-$ ,  $\text{Br}^-$ , and  
251  $\text{Li}^+$  was almost negligible and thus not further analyzed. Mass deposition of  $\text{Cl}^-$ ,  $\text{SO}_4^{2-}$ ,  $\text{Na}^+$  and  
252  $\text{Mg}^{2+}$  increased with elevation, and that of  $\text{NH}_4^+$  and  $\text{Ca}^{2+}$  increased with elevation except for the  
253 UCFL elevations. The increase of mass deposition with elevation can be explained by the rise of  
254 rain amount, which effectively deposits ions from the atmosphere into the surface. Mass deposition

255 of  $\text{PO}_4^{3-}$  and  $\text{K}^+$  did not have a clear pattern with elevation. Still, the deposition of  $\text{K}^+$  at the CFL  
256 and UCFL decreased, a behavior also seen by Medina et al. (2013). High inputs of  $\text{K}^+$  and  $\text{Mg}^{2+}$   
257 can be attributed to both marine and crustal sources (Valle-Díaz et al., 2016), while  $\text{PO}_4^{3-}$  can be  
258 attributed to crustal sources (Pett-Ridge, 2009). These results show that marine and crustal sources  
259 are the main contributors to the ion load and deposition to the Luquillo Mountains and that they  
260 are an important source of nutrients to the ecosystem.

261 The annual weighted mean concentration of ions was analyzed as a function of elevation (Fig. 5).  
262 This plot shows that the ion concentration at lower stations does not follow a clear trend but rather  
263 erratic movements. Similarly, the annual amount of rainfall did not follow a clear pattern. However,  
264 while the elevation between these stations is not large, their geographical location and exposure to  
265 the northeasterly trade winds are vastly different. The stations CDI, CDII, H, and PDM are located  
266 on the southeastern coast, while the stations LCD and LCM are situated in the most northeastern  
267 part of the island. This suggests that the trade winds and precipitation will more directly influence  
268 the latter two stations from marine cumulus clouds than those in the southeastern region. However,  
269 this is not necessarily the case as only the station CDII received less precipitation than those in the  
270 northeast. There is a clear difference in the total concentration of ions for these stations, with those  
271 located on the northeastern coast receiving more ions than those in the southeastern coast. The  
272 higher concentration of sea-salt ions ( $\text{Na}^+$ ,  $\text{Cl}^-$ ,  $\text{K}^+$  and  $\text{Mg}^{2+}$ ) in the northeastern coast stations  
273 suggests that the influence of the trade winds could be resulting in higher wind speeds that are  
274 dragging more marine aerosols with them. Also, these stations had the largest concentrations of  
275  $\text{SO}_4^{2-}$  because of the nearby mangroves that cause anoxic conditions in the ground and high  
276 sulfur content.

277 The lowland interior station Ford had the largest concentrations of  $K^+$ , and high concentrations of  
278  $PO_4^{3-}$  and  $NO_3^-$ , suggesting that these could be the results nearby manufacturing facilities and  
279 agricultural activity. The station JB had the highest values of  $nss-SO_4^{2-}$  from the lowland interior  
280 stations, which is expected because this station is in the highly populated metropolitan area and  
281 more exposed to the aerosols emitted from anthropogenic activity.

282 Stations in the LM, CFL and UCFL areas showed a more consistent trend of increasing  
283 precipitation and decreasing ion concentration. The clearest exceptions to this trend were the ELV  
284 and Toro stations that had a noticeably lower amount of rainfall than the rest of the stations in its  
285 altitude classification. Interestingly, these stations are in the western part of the mountains. Since  
286 the mountain formation is close to the coast and has a steep elevation slope, they are prone to form  
287 precipitation due to orographic lifting of air masses moved by the trade winds. Those stations in  
288 the western part of the mountain will experience the rain shadow effect, where most of the  
289 precipitation forms in the eastern face of the mountain. The Toro station is further west than the  
290 rest of the mountain stations and thus experiences this effect more, reflected in the reduced  
291 precipitation and increased ion concentration compared to the rest of the stations at comparable  
292 altitudes. This station also presented higher  $nss-SO_4^{2-}$  and  $PO_4^{3-}$  than the rest of the mountain  
293 stations, suggesting that there could be emissions from primary biogenically aerosols being emitted  
294 in the forest and reaching this station. Anthropogenic activity in this area is unlikely since it is part  
295 of a protected area where no development is allowed. Another exception to this trend is the UCFL  
296 stations, where the concentration of aerosols exponentially increased for the MB, PEC and POC  
297 stations and drops for the YPC station. The ions that followed this countertrend were the marine  
298 aerosols  $Na^+$ ,  $Cl^-$  and  $Mg^{2+}$ , along with  $NO_3^-$  and  $PO_4^{3-}$ . An explanation for this behavior was not  
299 found. A possible reason for the decrease in precipitation at the YPC station relative to the trend

300 that the other stations in its altitude range follow could be that this station is slightly higher than  
301 where most precipitation forms and being excluded from some of the rain events.

302 The ion concentration results from this study were higher for all species than those reported in  
303 Medina et al. (2013). However, our dataset comprises a more extended period and is more  
304 representative of the average yearly deposition at the different locations, as well as including  
305 periods of abnormally low rainfall, as in the case of 2015, where concentrations increase. Asbury  
306 et al. (1994) determined ion concentrations at Pico del Este that were 2.5 to 5.5 times higher than  
307 the concentration determined in this study for UCFL stations, like the observation made in Medina  
308 et al. (2013). The results from Gioda et al. (2011) from seven rain events at Pico del Este agree  
309 well with ours, although slightly lower for most ions except  $\text{NO}_3^-$  and  $\text{SO}_4^{2-}$ , which we attribute is  
310 because this sampling took place during the winter period where cold fronts carrying  
311 anthropogenic pollution are common. Gioda et al. (2013) analyzed ions in rainwater at three  
312 locations of the Luquillo Mountain: El Verde, Bisley, and Pico del Este. Our results of ELV agree  
313 well with their results for the same El Verde area, except for the case of  $\text{K}^+$  and  $\text{NH}_4^+$ , for which  
314 we got an average concentration about a factor 4 and 10 higher, respectively, and  $\text{NO}_3^-$  where we  
315 got an about a factor 12 lower concentration. In Pico del Este (PEC), for  $\text{Ca}^{2+}$ ,  $\text{Mg}^{2+}$ ,  $\text{K}^+$ , and  $\text{SO}_4^{2-}$   
316 we got about a factor 2 lower concentrations, slightly lower concentrations for  $\text{Na}^+$  and  $\text{Cl}^-$ ,  
317 drastically lower concentration for  $\text{NO}_3^-$  and only  $\text{NH}_4^+$  agreed well in both studies. Differences in  
318 concentrations determined at PEC may have arisen from not being in the same location and being  
319 possibly exposed to different weather conditions, as well as by different sample collection and  
320 analysis methodology. A more recent study of a 20-yr record of rain chemistry at Bisley and El  
321 Verde by McClintock et al. (2019) showed concentrations of  $\text{nss-Ca}^{2+}$  lower than those presented  
322 here.

323 A considerable difference from our work is that most of these studies collected one-week samples  
324 or samples by rain events for their analysis, while our samples were from two weeks. The  
325 additional time in the field can cause differences in the ion concentrations as they are exposed to  
326 daily changes in temperature, and as redox reactions take place. We expect this effect to be higher  
327 in lower elevation station as temperatures decrease with elevation. Also, these samples are more  
328 prone to have enhanced concentration of ions due to dry deposition of aerosol particles, which  
329 would explain the higher concentration of specific ions in this study in comparison to those who  
330 have a shorter hold time in the field. Medina et al. (2013) estimated an enhancement of up to 40%  
331 in  $\text{Na}^+$  and  $\text{Cl}^-$  concentrations and up to 60% in  $\text{Mg}^{2+}$  and  $\text{Ca}^{2+}$  concentration in comparison to the  
332 National Atmospheric Deposition Program (NADP) samples collected at lower montane stations.

333 When the results from this study are compared with those of other rainforest, the effect of the air  
334 mass influence on the rain chemistry becomes more apparent. A study done in West Africa by  
335 Sigha-Nkamdjou et al., 2003 reported that their most abundant inorganic ions were  $\text{NH}_4^+$  and  $\text{NO}_3^-$   
336 corresponding to biomass burning aerosols and low abundance of  $\text{Na}^+$  and  $\text{Cl}^-$ , that were the most  
337 abundant ions in our study. Concentrations of  $\text{NH}_4^+$  and  $\text{NO}_3^-$  were about 3 times larger and 6 times  
338 lower, respectively in our study while concentrations of  $\text{Na}^+$  and  $\text{Cl}^-$  were substantially higher. A  
339 study done in a tropical forest in eastern China influenced by emissions from motor vehicles by  
340 Niu et al., 2017 found that  $\text{SO}_4^{2-}$  and  $\text{NO}_3^-$  accounted for about 88% of their inorganic ion  
341 composition. The volume weighted mean values for both of this species were 49.8 and 32.6  $\mu\text{eq}$   
342  $\text{L}^{-1}$ , respectively, that were 25 and 97% larger than the maximum concentration seen in this study.

343 Our results are much more comparable to those found in Lesack and Melack, 1991 where rain  
344 chemistry was studied in the tropical forest of La Selva, Costa Rica. This study found that the  
345 largest ion influence in rainwater was from marine sources, although our study reported larger

346 concentrations of marine aerosols. We also saw an overall higher concentration of all ions than  
347 what Lesack and Melack, 1991 reported, which could be due to differences in location and  
348 sampling methodology, which can also explain differences with the other studies.

349

## 350 **CONCLUSION**

351

352 A rich multiyear dataset of rainfall amount and chemical composition along the elevation gradient  
353 of the Luquillo Mountains was analyzed. Contrary to what other studies report (Torres-Valcárcel  
354 et al., 2014; Van Beusekom et al., 2015), we found that for most stations, the amount of rainfall  
355 has been decreasing over the past years up until 2015 and then increased for the last three years.

356 A decrease in precipitation could mean a future negative outcome for the ecosystem that depends  
357 on high water inputs yearlong. However, the present is a short-term study and unable to assess any  
358 climatic pattern, but these results can help forest managers make timely decisions to preserve  
359 biodiversity in the most vulnerable ecosystems.

360 A positive correlation was found between elevation and rainfall, although not all stations followed  
361 this behavior. This suggests that ecosystems at higher altitudes (CFL and UCFL) could be more  
362 affected by changes in precipitation inputs, such as the elfin cloud forest found at the most upper  
363 parts of the Luquillo Mountains. There was not a clear pattern of pH with rainfall, but an inverse  
364 exponential relationship between the total ion concentration and the total rainfall was found.

365 Ion composition was shown to be dependent on transported aerosols and have a clear seasonal  
366 pattern. While marine aerosols are present year-round, crustal aerosols are more abundant during  
367 the summer period and anthropogenic aerosols during the winter period. Particularly, crustal



368 aerosols from the influence of African dust are an important source of micro and macronutrients,  
369 providing calcium, phosphate, and other nutrients along the gradient.

370 While it is expected that rainfall would increase and ion concentration would decrease with  
371 elevation, this was not always the case. The Luquillo Mountains have a complex topography that  
372 largely influences cloud formation and precipitation patterns. Because of this, the elevation is not  
373 a sole predictor of these variables, but location along the mountain proved to be important.  
374 Montane stations located to the west of the mountain range usually experienced lower rainfall  
375 amounts and higher ion concentration than stations in its elevation range, but that where further  
376 east because of the rain shadow effect. Ion deposition usually increased with elevation for most  
377 ions, indicating that rainfall is an essential source of both water and nutrients to montane  
378 ecosystems.

379

## 380 **ACKNOWLEDGMENTS**

381

382 The authors thank Carlos Estrada, Samuel Moya, Humberto Robles, and Carlos Torrens for  
383 assisting with field data collection, and personnel of the International Institute of Tropical Forestry  
384 Chemistry Laboratory for water chemistry analyses. The authors also acknowledge Ariel E. Lugo  
385 for reviewing an earlier draft of the manuscript. This research was funded by the Luquillo Critical  
386 Zone Observatory (National Science Foundation grant EAR-1331841), Luquillo Long-Term  
387 Ecological Research Site (National Science Foundation grant DEB-1239764), and the USDA  
388 Forest Service. The authors acknowledge the USDA Natural Resources Career Program (Grant  
389 2017-38422-27131) for student financial support during this project. All research at the

390 International Institute of Tropical Forestry is done in collaboration with the University of Puerto  
391 Rico. Any use of trade, product, or firms' names is for descriptive purposes only and does not  
392 imply endorsement by the U.S. Government.

393

#### 394 **DISCLAIMER**

395 Reference to any companies or specific commercial products does not constitute an endorsement  
396 from authors.

397

#### 398 **REFERENCES**

399

- 400 Allan, J.D., Baumgardner, D., Raga, G.B., Mayol-Bracero, O.L., Morales-García, F., García-  
401 García, F., Montero-Martínez, G., Borrmann, S., Schneider, J., Mertes, S., Walter, S.,  
402 Gysel, M., Dusek, U., Frank, G.P., Krämer, M., 2008. Clouds and aerosols in Puerto Rico -  
403 A new evaluation. *Atmos. Chem. Phys.* **8**, 1293–1309. [https://doi.org/10.5194/acp-8-1293-](https://doi.org/10.5194/acp-8-1293-2008)  
404 2008
- 405 Asbury, C.E., McDowell, W.H., Trinidad-Pizarro, R., Berrios, S., 1994. Solute deposition from  
406 cloud water to the canopy of a puerto rican montane forest. *Atmos. Environ.* **28**, 1773–  
407 1780. [https://doi.org/10.1016/1352-2310\(94\)90139-2](https://doi.org/10.1016/1352-2310(94)90139-2)
- 408 Brokaw, N., Crowl, T.A., Lugo, A.E., McDowell, W.H., Scatena, F.N., Waide, R.B., Willig,  
409 M.R., 2012. *A Caribbean forest tapestry: the multidimensional nature of disturbance and*  
410 *response*. New York: Oxford University Press.

411 García-Martinó, A.R., Warner, G.S., Scatena, F.N., Civco, D.L., 1996. Rainfall, Runoff and  
412 Elevation Relationships in the Luquillo Mountains of Puerto Rico\*. *Caribb. J. Sci.* **32**, 41–  
413 65.

414 Gioda, A., Mayol-Bracero, O.L., Morales-García, F., Collett, J., Decesari, S., Emblico, L.,  
415 Facchini, M.C., Morales-De Jesús, R.J., Mertes, S., Borrmann, S., Walter, S., Schneider, J.,  
416 2009. Chemical composition of cloud water in the puerto rican tropical trade wind cumuli.  
417 *Water. Air. Soil Pollut.* **200**, 3–14. <https://doi.org/10.1007/s11270-008-9888-4>

418 Gioda, A., Mayol-Bracero, O.L., Scatena, F.N., Weathers, K.C., Mateus, V.L., McDowell, W.H.,  
419 2013. Chemical constituents in clouds and rainwater in the Puerto Rican rainforest:  
420 Potential sources and seasonal drivers. *Atmos. Environ.* **68**, 208–220.  
421 <https://doi.org/10.1016/j.atmosenv.2012.11.017>

422 Gioda, A., Reyes-Rodríguez, G.J., Santos-Figueroa, G., Collett, J.L., Decesari, S., Ramos,  
423 M.D.C.K.V., Bezerra Netto, H.J.C., De Aquino Neto, F.R., Mayol-Bracero, O.L., 2011.  
424 Speciation of water-soluble inorganic, organic, and total nitrogen in a background marine  
425 environment: Cloud water, rainwater, and aerosol particles. *J. Geophys. Res. Atmos.* **116**.  
426 <https://doi.org/10.1029/2010JD015010>

427 González, G., Willig, M.R., Waide, R.B., 2013. Ecological gradient analyses in a tropical  
428 landscape. *Ecological Bulletins* **54**. Hoboken, NJ: Wiley-Blackwell, p. 252.

429 Gould, W.A., González, G., Rivera, G.C., 2006. Structure and Composition of Vegetation along  
430 an Elevational Gradient in Puerto Rico. *J. Veg. Sci.* <https://doi.org/10.2307/4096714>

431 Heartsill-Scalley, T., Scatena, F.N., Estrada, C., McDowell, W.H., Lugo, A.E., 2007.  
432 Disturbance and long-term patterns of rainfall and throughfall nutrient fluxes in a

433 subtropical wet forest in Puerto Rico. *J. Hydrol.* **333**, 472–485.  
434 <https://doi.org/10.1016/j.jhydrol.2006.09.019>

435 Lesack, L.F.W., Melack, J.M., 1991. The Deposition, Composition, and Potential Sources of  
436 Major Ionic Solutes in Rain of the Central Amazon Basin. *Water Resour. Res.* **27**, 2953–  
437 2977. <https://doi.org/10.1029/91WR01946>

438 Lugo, A.E., Waide, R.B., Willig, M.R., Crowl, T.A., Scatena, F.N., Thompson, J., Silver, W.L.,  
439 McDowell, W.H., Brokaw, N., 2015. Ecological Paradigms for the Tropics: Old Questions  
440 and Continuing Challenges, in: *A Caribbean Forest Tapestry: The Multidimensional Nature*  
441 *of Disturbance and Response*. Oxford University Press.  
442 <https://doi.org/10.1093/acprof:osobl/9780195334692.003.0001>

443 Manahan, S., 2000. *Fundamentals of Environmental Chemistry, Second Edition, Fundamentals*  
444 *of Environmental Chemistry, Second Edition*. CRC Press.  
445 <https://doi.org/10.1201/9781420056716>

446 Martens, C.S., Harriss, R.C., 1973. Chemistry of aerosols, cloud droplets, and rain in the Puerto  
447 Rican marine atmosphere. *J. Geophys. Res.* **78**, 949–957.  
448 <https://doi.org/10.1029/jc078i006p00949>

449 McClintock, M.A., McDowell, W.H., González, G., Schulz, M., Pett-Ridge, J.C., 2019. African  
450 dust deposition in Puerto Rico: Analysis of a 20-year rainfall chemistry record and  
451 comparison with models. *Atmos. Environ.* **116907**.  
452 <https://doi.org/10.1016/j.atmosenv.2019.116907>

453 McDowell, W.H., Sánchez, C.G., Asbury, C.E., Ramos Pérez, C.R., 1990. Influence of sea salt  
454 aerosols and long range transport on precipitation chemistry at El Verde, Puerto Rico.

455 Atmos. Environ. Part A, Gen. Top. **24**, 2813–2821. <https://doi.org/10.1016/0960->  
456 1686(90)90168-M

457 Medina, E., González, G., Rivera, M.M., 2013. Spatial and temporal heterogeneity of rainfall  
458 inorganic ion composition in northeastern Puerto Rico. *Ecological Bull.* **54**, 157–167.

459 Murphy, S.F., Stallard, R.F., Scholl, M.A., González, G., Torres-Sánchez, A.J., 2017.  
460 Reassessing rainfall in the Luquillo Mountains, Puerto Rico: Local and global  
461 ecohydrological implications. *PLoS One* **12**. <https://doi.org/10.1371/journal.pone.0180987>

462 Niu, Y., Li, X., Huang, Z., Zhu, C., 2017. Chemical characteristics and possible causes of acid  
463 rain at a regional atmospheric background site in eastern China. *Air Qual. Atmos. Heal.* **10**,  
464 971–980. <https://doi.org/10.1007/s11869-017-0486-8>

465 Odum, H.T., 1970. Summary: an emerging view of the ecological system at El Verde. Odum, H.  
466 T., *Tropical rain forest Bibliography*, p.277-281.

467 Pett-Ridge, J.C., 2009. Contributions of Dust to Phosphorus Cycling in Tropical Forests of the  
468 Luquillo Mountains, Puerto Rico. *Biogeochemistry*, **94**, 63-80.  
469 <https://doi.org/10.2307/20519864>

470 Prospero, J.M., Lamb, P.J., 2003. African Droughts and Dust Transport to the Caribbean:  
471 Climate Change Implications. *Science*. **302**, 1024–1027.  
472 <https://doi.org/10.1126/science.1089915>

473 Prospero, J.M., Mayol-Bracero, O.L., 2013. Understanding the transport and impact of African  
474 dust on the Caribbean Basin. *Bull. Am. Meteorol. Soc.* **94**, 1329–1337.  
475 <https://doi.org/10.1175/BAMS-D-12-00142.1>

476 Sigha-Nkamdjou, L., Galy-Lacaux, C., Pont, V., Richard, S., Sighomnou, D., Lacaux, J.P., 2003.  
477 Rainwater chemistry and wet deposition over the equatorial forested ecosystem of Zoétélé  
478 (Cameroon). *J. Atmos. Chem.* **46**, 173–198. <https://doi.org/10.1023/A:1026057413640>

479 Stallard, R.F., Murphy, S.F., 2012. Atmospheric Inputs to Watersheds of the Luquillo Mountains  
480 in Eastern Puerto Rico Water Quality and Landscape Processes of Four Watersheds in  
481 Eastern Puerto Rico, in: Murphy, Sheila F.; Stallard, R.F. (Ed.), *Water Quality and*  
482 *Landscape Processes of Four Watersheds in Eastern Puerto Rico*. pp. 89–109.

483 Torres-Valcárcel, Á., Harbor, J., González-Avilés, C., Torres-Valcárcel, A., 2014. Impacts of  
484 urban development on precipitation in the tropical maritime climate of puerto rico. *Climate*  
485 **2**, 47–77. <https://doi.org/10.3390/cli2020047>

486 Valle-Díaz, C.J., Torres-Delgado, E., Colón-Santos, S.M., Lee, T., Collett, J.L., McDowell,  
487 W.H., Mayol-Bracero, O.L., 2016. Impact of long-range transported african dust on cloud  
488 water chemistry at a tropical montane cloud forest in Northeastern Puerto Rico. *Aerosol Air*  
489 *Qual. Res.* **16**, 653–664. <https://doi.org/10.4209/aaqr.2015.05.0320>

490 Van Beusekom, A.E., González, G., Rivera, M.M., 2015. Short-Term Precipitation and  
491 Temperature Trends along an Elevation Gradient in Northeastern Puerto Rico. *Earth*  
492 *Interact. d* **19**. <https://doi.org/10.1175/EI-D-14-0023.1>

493 Weathers, K.C., Likens, G.E., Herbert Bormannrbert, F., Bicknell, S.H., Bormann, B.T., Daube,  
494 B.C., Eaton, J.S., Galloway, J.N., Keene, W.C., Kimball, K.D., McDowell, W.H., Siccama,  
495 T.G., Smiley, D., Tarrant, R.A., 1988. Cloudwater Chemistry from ten Sites in North  
496 America. *Environ. Sci. Technol.* **22**, 1018–1026. <https://doi.org/10.1021/es00174a004>

497

498 **Table 1:** Description and geographical information of collection stations.

Station Name	Station ID	Elevation (m)	Elevation site	Latitude (N)	Longitude (W)
Palmas del Mar	PDM	0	Lowland coastal	18°05'32.63"	65°48'04.64"
Humacao	H	3	Lowland coastal	18°10'42.27"	65°45'53.23"
Sabana Seca #2	SS#2	3	Lowland coastal	18°27'40.45"	66°12'16.65"
Las Cabezas II	LCM	4	Lowland coastal	18°22'40.73"	65°37'08.90"
Ceiba I	CDI	9	Lowland coastal	18°13'59.01"	65°35'59.13"
Ceiba II	CDII	14	Lowland coastal	18°13'15.13"	65°40'13.43"
Las Cabezas I	LCD	31	Lowland coastal	18°22'51.29"	65°37'13.71"
Ford	Ford	13	Lowland interior	18°23'12.23"	65°52'48.04"
Jardín Botánico	JB	26	Lowland interior	18°23'01.35"	66°03'11.30"
Saint Just	SJ	81	Lowland interior	18°23'04.90"	65°59'58.23"
Sabana 4 Bisley	S4	226	Lower Montane	18°19'01.63"	65°44'30.68"
Sabana 4 Bisley #2	S4#2	226	Lower Montane	18°19'01.63"	65°44'30.68"
El Verde	ELV	361	Lower Montane	18°19'10.02"	65°48'58.28"
Rio Grande	RG	525	Lower Montane	18°17'36.83"	65°48'23.47"
UPR (Nido)	NIDO	655	Cloud Formation Level	18°18'00.81"	65°47'00.05"
Pico del Este I - Colorado	CO	778	Cloud Formation Level	18°17'38.58"	65°47'11.46"
El Toro	TORO	792	Cloud Formation Level Upper Cloud	18°16'40.06"	65°50'53.26"
Mount Britton	MB	901	Formation Level Upper Cloud	18°18'16.02"	65°47'26.14"
Pico del Oeste	POC	987	Formation Level Upper Cloud	18°16'39.18"	65°45'51.44"
Pico del Este II - Cloud	PEC	1002	Formation Level Upper Cloud	18°16'17.15"	65°45'40.42"
El Yunque	YPC	1045	Formation Level	18°18'38.23"	65°45'26.14"

499  
500  
501

502

503

504

505

506

507

508

509

510 **Table 2:** Pearson correlation factor for different ions. Values in bold represent highly significant  
 511 correlation (>0.7). Values in parenthesis represents correlation with non-sea salt fraction of the  
 512 species.

Station	Pearson Correlation Factor			n
	Na <sup>+</sup> vs Cl <sup>-</sup>	Na <sup>+</sup> vs Ca <sup>2+</sup> (nss-Ca <sup>2+</sup> )	Na <sup>+</sup> vs SO <sub>4</sub> <sup>2-</sup> (nss-SO <sub>4</sub> <sup>2-</sup> )	
PDM	0.49	0.445 (0.599)	0.496 (0.095)	64
H	<b>0.781</b>	0.312 (0.424)	<b>0.745</b> (0.285)	59
SS#2	<b>0.948</b>	0.332 (0.496)	<b>0.749 (0.759)</b>	32
LCM	<b>0.718</b>	0.358 (0.344)	0.634 (0.154)	63
CDI	<b>0.949</b>	<b>0.784</b> (0.430)	<b>0.779</b> (0.209)	63
CDII	0.693	0.584 (0.469)	<b>0.703</b> (0.347)	62
LCD	<b>0.948</b>	0.397 ( <b>0.799</b> )	0.179 (0.126)	61
Ford	0.699	0.187 (0.582)	0.649 (0.194)	65
JB	<b>0.737</b>	0.35 (0.260)	0.592 (0.499)	65
SJ	0.569	0.288 (0.210)	<b>0.792</b> (0.398)	66
S4	<b>0.891</b>	0.021 (-0.031)	<b>0.712</b> (-0.027)	70
S4#2	<b>0.851</b>	0.113 (-0.108)	0.65 (-0.434)	38
ELV	<b>0.907</b>	0.134 (0.090)	<b>0.732</b> (-0.044)	70
RG	<b>0.922</b>	0.158 (0.231)	0.599 (0.617)	70
NIDO	<b>0.901</b>	0.169 (0.181)	<b>0.778</b> (0.413)	70
CO	<b>0.896</b>	0.144 (0.093)	<b>0.802</b> (0.167)	70
TORO	<b>0.911</b>	0.564 (0.413)	0.609 (-0.138)	70
MB	<b>0.895</b>	0.246 (0.176)	<b>0.751</b> (0.188)	70
POC	<b>0.833</b>	0.145 (0.036)	<b>0.757</b> (0.097)	70
PEC	<b>0.907</b>	0.089 (0.028)	<b>0.785</b> (0.096)	69
YPC	<b>0.92</b>	0.248 (0.157)	<b>0.768</b> (0.377)	68

513  
 514  
 515  
 516  
 517  
 518  
 519  
 520  
 521



522 **Table 3:** Yearly ion mass deposition per unit area for the different elevation groups.

Elevation Group	Ion Deposition (kg/ha/year)											
	Fl <sup>-</sup>	Cl <sup>-</sup>	SO <sub>4</sub> <sup>2-</sup>	Br <sup>-</sup>	NO <sub>3</sub> <sup>-</sup>	PO <sub>4</sub> <sup>3-</sup>	Li <sup>+</sup>	Na <sup>+</sup>	NH <sub>4</sub> <sup>+</sup>	K <sup>+</sup>	Mg <sup>++</sup>	Ca <sup>++</sup>
LC	0.290	34.0	7.64	0.280	0.140	3.33	0.070	17.8	2.06	8.10	2.91	4.38
LI	0.200	32.9	8.73	0.180	0.240	3.49	0.077	16.2	3.07	12.9	2.55	5.84
LM	0.238	44.0	10.6	0.198	0.238	2.69	0.188	25.9	3.39	7.22	3.40	5.19
CFL	0.237	61.2	16.6	0.263	0.310	5.50	0.173	31.9	4.44	7.05	4.28	7.01
UCFL	0.200	70.4	18.8	0.218	0.515	4.74	0.225	40.0	2.38	3.47	4.90	5.93

523

524

525

526

527

528

529

530

531

532

533

534

535

536

537

538

539 **Figure Captions**

540 **Fig 1:** Annual averages of rainfall as a function of elevation for all sampling sites.

541 **Fig 2:** Monthly profile of rainfall by elevation type. Error bars correspond to standard deviation.

542 Lines are slightly offset for easier viewing.

543 **Fig 3:** Linear regression analysis of the natural logarithm of total ion concentration as a function  
544 of the natural logarithm of rainfall.

545 **Fig 4:** Monthly profile of calcium, sulfate, and sodium concentration at different elevation types.

546 **Fig 5:** Yearly weighted means ion concentration for each station.

547

548

549

550

551

552

553

554

555

556

557

558

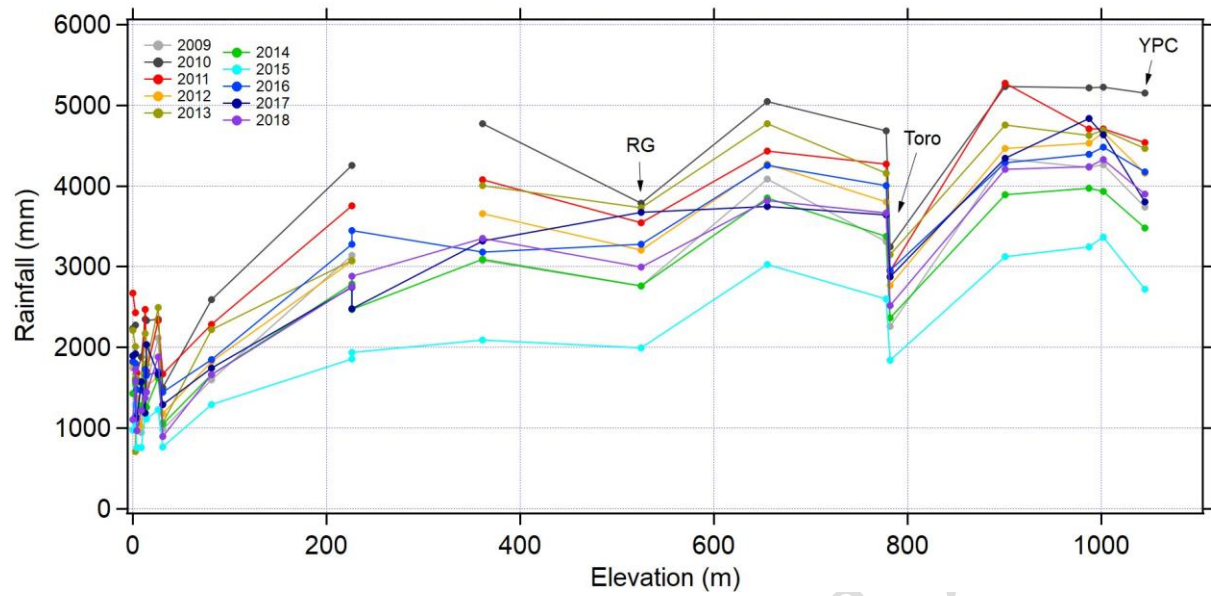
559

560

561

562

563



564

565 **Fig 1:** Annual averages of rainfall as a function of elevation for all sampling sites.

566

567

568

569

570

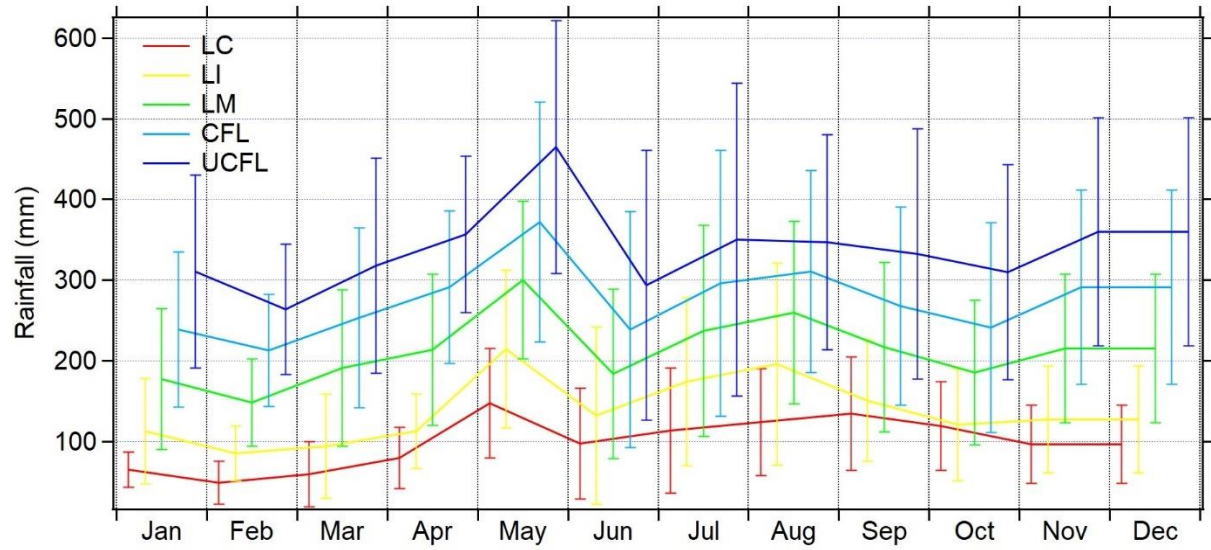
571

572

573

574

ACCEPTED MANUSCRIPT



575  
 576 **Fig 2:** Monthly profile of rainfall by elevation type. Error bars correspond to standard deviation.

577 Lines are slightly offset for easier viewing.

578

579

580

581

582

583

584

585

586

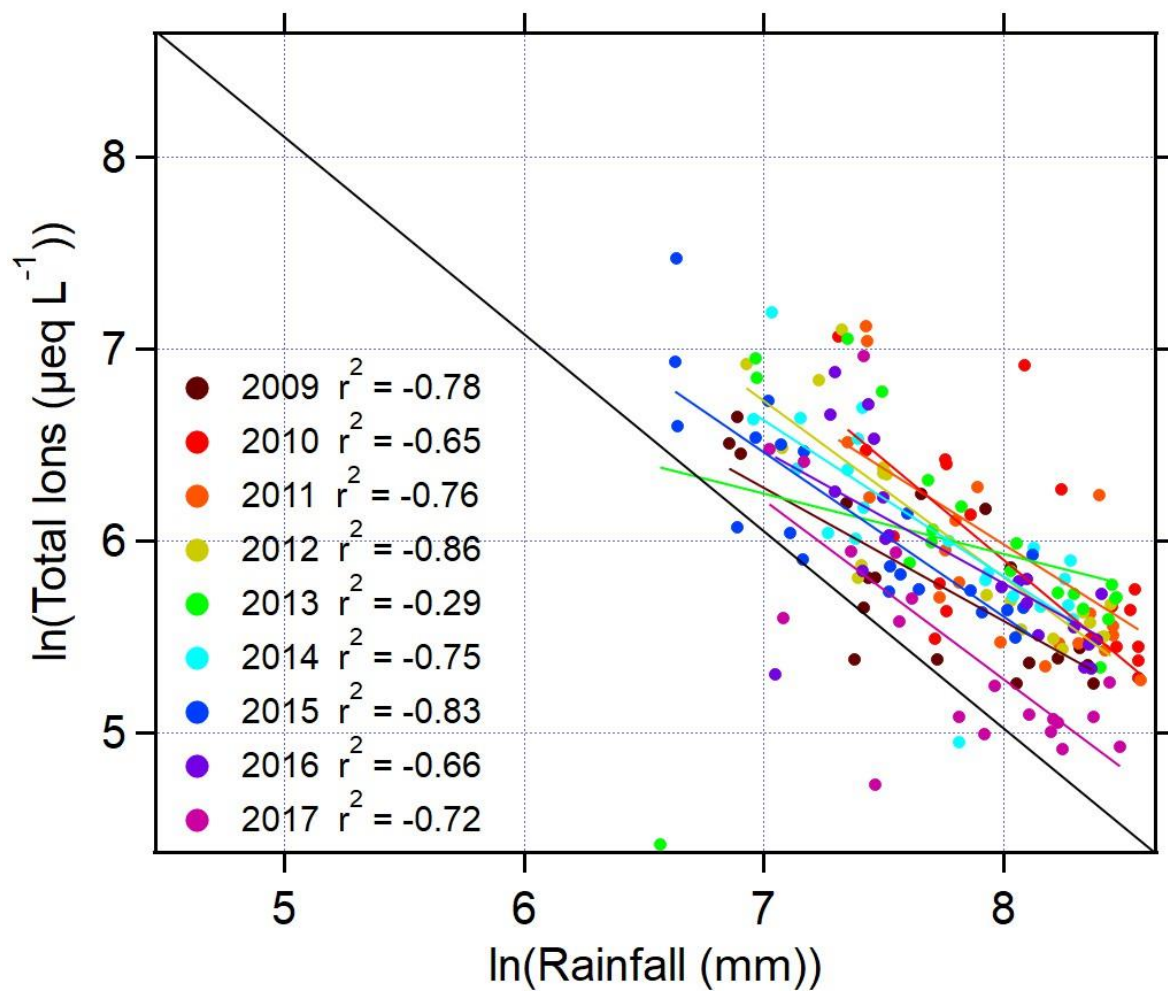
587

588

589

590

591



592

593 **Fig 3:** Linear regression analysis of the natural logarithm of total ion concentration as a function

594 of the natural logarithm of rainfall.

595

596

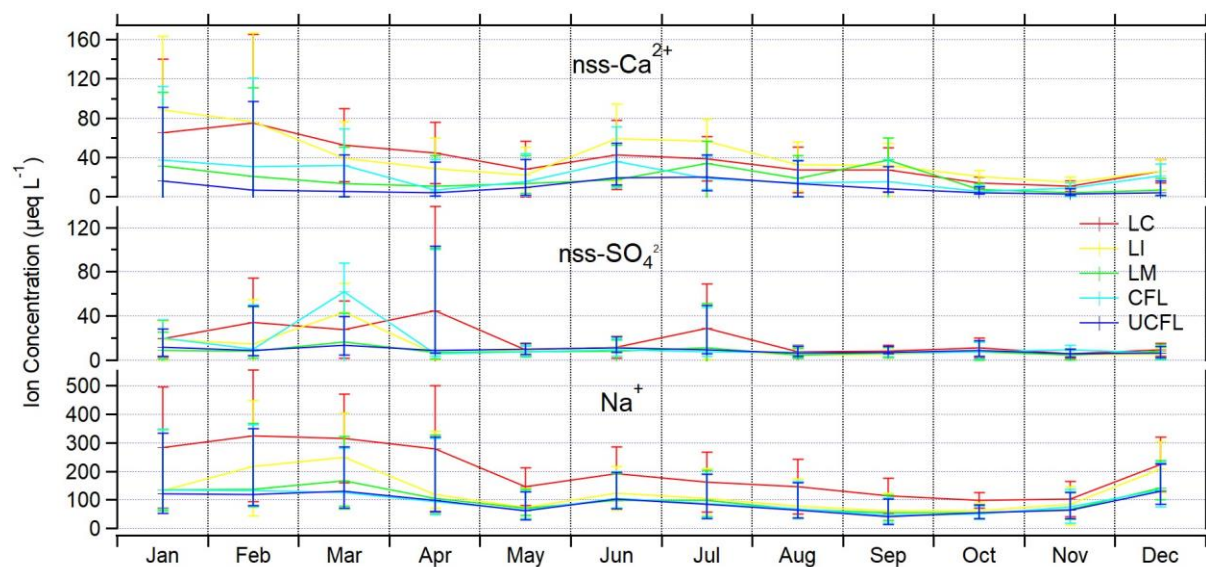
597

598

599

600

601



602

603 **Fig 4:** Monthly profile of non-sea salt calcium, non-sea salt sulfate, and sodium concentration at  
 604 different elevation types.

605

606

607

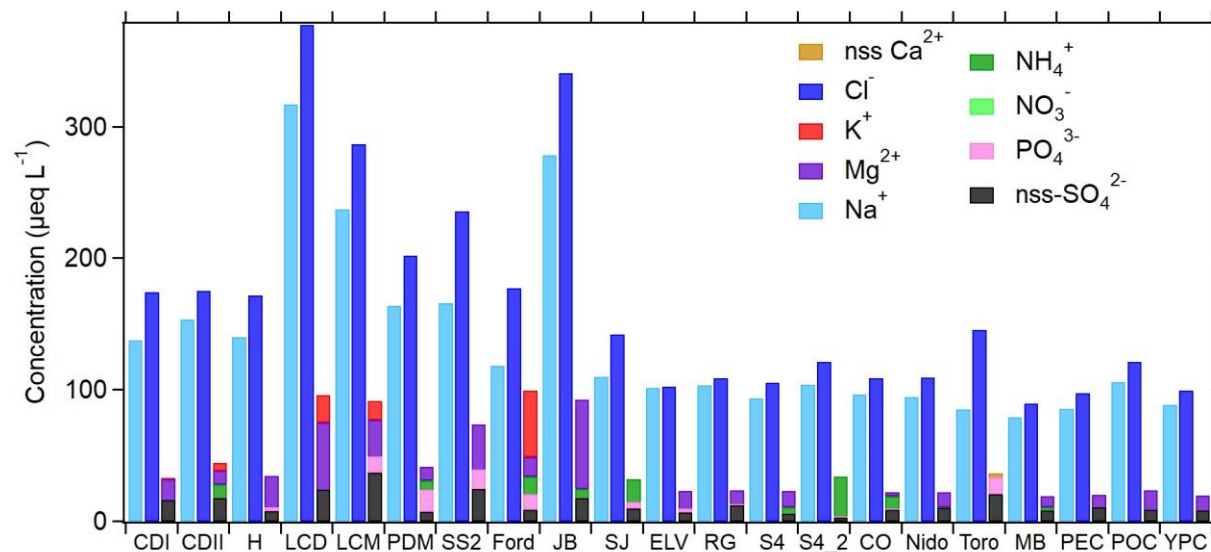
608

609

610

611

ACCEPTED MANUSCRIPT



612

613 **Fig 5:** Yearly weighted means ion concentration for each station.

ACCEPTED MANUSCRIPT